

# PROCEEDINGS OF SPIE

[SPIDigitalLibrary.org/conference-proceedings-of-spie](https://spiedigitallibrary.org/conference-proceedings-of-spie)

## Short-pulse laser propagation through tissues

Champak Das  
Ashish Trivedi  
Kunal Mitra  
Tuan Vo-Dinh

**SPIE.**

# Short Pulse Laser Propagation Through Tissues

Champak Das<sup>a</sup>, Ashish Trivedi<sup>a</sup>, Kunal Mitra<sup>\*a</sup>, Tuan Vo-Dinh<sup>\*\*b</sup>  
<sup>a</sup>Florida Institute of Technology; <sup>b</sup>Oak Ridge National Laboratory

## ABSTRACT

An experimental and numerical study is performed to analyze short pulse laser propagation through tissue phantoms without and with inhomogeneities / tumors imbedded in it. Short pulse laser probing techniques has distinct advantages over conventional very large pulse width or cw lasers primarily due to the additional information conveyed about the tissue interior by the temporal variation of the observed signal. Both the scattered temporal transmitted and reflected optical signals are measured experimentally using a streak camera for samples irradiated with a short pulse laser source. Parametric study involving different scattering and absorption coefficients of tissue phantoms and inhomogeneities as well as the detector position and orientation is performed. The temporal and spatial profiles of the scattered optical signals are compared with the numerical modeling results obtained by solving the transient radiative transport equation using discrete ordinates technique.

**Keywords:** short pulse laser, transient radiative transfer, tumor, tissues, detection

## 1. INTRODUCTION

The study of short pulse laser radiation transport through highly scattering media has received increasing attention during last few years as a result of its wide applications such as optical imaging for medical diagnosis,<sup>1-4</sup> surgical and therapeutics,<sup>5-8</sup> remote sensing,<sup>9,10</sup> and material processing.<sup>11</sup> The nascent field of optical tomography for biomedical imaging using short pulse laser is made possible by a spectral window in the infrared wavelength region where light absorption is very small and scattering dominates.<sup>3,12-14</sup> Optical methods are a recent addition to the arsenal of non-invasive diagnostic tools available for the detection of disease, such as x-ray computed tomography, magnetic resonance imaging, positron emission tomography, single photon emission computed tomography, ultrasound imaging, and electrical impedance tomography. In optical tomography a short pulse laser is focused on the region to be probed and the time-dependent scattered reflected and transmitted signals are measured at different locations using ultrafast detectors. It is the intent of the method to reconstruct the image of the interior and determine optical properties of the tissue medium from the time-resolved intensity measurements.

Short pulse laser probing techniques for diagnostics have distinct advantages over very large pulse width or continuous wave lasers primarily due to the additional information conveyed by the temporal distribution of the observed signal.<sup>15,16</sup> The distinct feature is the multiple scattering induced temporal distributions which persists for a time period greater than the duration of the source pulse and is a function of the source pulse width as well as the optical properties of the medium. If the detection is carried out at the same short time scale (comparable to the order of the pulse width), the signal continues to be observed even at large times after the pulse has been off due to the time taken for the photons to migrate to the detector after multiple scattering in the media. Forward and backward radiative transport models for determination of optical properties of the tissue interior from transmitted and reflected signal measurements can therefore be based on the full temporal signal.<sup>17-19</sup> Moreover, steady state measurements are somewhat cumbersome because it requires several independent measurements at different source-detector spacing to yield the optical properties of interest.

Another technique that is commonly used for biomedical imaging focuses on the initial transients of the temporal signal. Short laser pulses traversing through discrete scattering media is considered to be split into ballistic (coherent) and diffuse (incoherent) components.<sup>20</sup> If only the earliest arriving photons are collected by an appropriate gating technique,

\* kmitra@fit.edu; 150 W. University Blvd., Melbourne, FL 32901; phone: (321) 674 7131; fax: (321) 674 8813

\*\* vodinh@ornl.gov; P.O. Box 2008, M.S. 6101, Oak Ridge, TN 37831-6101; phone: (865) 574 6249; fax: (865) 576 7651

the direct line of sight property variations can be inferred since the earliest arriving photons correspond to those traveling the shortest optical path between the source and detector.<sup>21,22</sup> The photons detected first have been deviated least from the optical axis and the intensity measured over a small period depends on the optical properties of the region contained within a small volume surrounding optical axis. Time gating,<sup>23</sup> space gating,<sup>24,25</sup> holographic gating or optical coherence interferometry techniques,<sup>26</sup> and streak camera applications<sup>27</sup> have been used for evaluating the earliest arriving photons. However, these ballistic components may not be of practical use for tissues thicker than a few centimeters because they are not measurable with increasing tissue thickness.

In addition to the time-resolved measurement technique, frequency domain techniques have been also developed to acquire transmitted light information in the frequency domain directly. A significant disadvantage of the frequency domain method, though generally a less expensive method, is that sources that can provide significant power at very high frequencies are not yet available. Most experimental work performed so far has utilized frequencies of a few hundred megahertz, which is equivalent to a temporal resolution of a few nanoseconds, and photon density wavelengths of the order of a meter.<sup>28-30</sup> It has been reported in the literature that there is a need for high modulation frequencies to obtain images with high resolution when imaging tissues having particularly low average absorption and high scattering coefficients.<sup>31</sup>

In order to predict the optical properties of tissues from time-resolved scattered signal measurements development of inverse algorithm is required. Before development of complex inverse algorithms, accurate forward solutions of transient radiative transport equation necessary to analyze short pulse laser propagation through tissues is critical. In most previous analysis, the transient term of the radiative transport equation (RTE) is usually neglected. This assumption does not lead to errors as the temporal variations of observed signals are slow compared to the time of flight of a photon. However, in applications involving short pulsed laser interactions with tissues, the transient effect must be considered in the RTE.<sup>1,3,15,32,33</sup>

Transient solution of radiative transfer equation for one-dimensional geometry for the case of short pulse laser incidence has been developed and reported in the literature.<sup>1,15,34-36</sup> The work has been extended to two-dimensional geometry using the simplified first order spherical harmonics ( $P_1$ ) approximation for a rectangular geometry.<sup>37</sup> Integral equation formulation techniques for the transient radiative transport equation have been also developed.<sup>38,39</sup> However, the  $P_1$  model underestimates the speed of light propagation<sup>1,15</sup> and the integral formulation is difficult to be applied to complex geometries. Monte Carlo (MC) method has been also used by many researchers.<sup>40,41</sup> The MC method requires a large number of emitted bundles to obtain smooth accurate solutions which is computationally expensive. The discrete ordinate method (DOM) has become popular for solving transient radiative transport equation accurately and efficiently. The one-dimensional DOM has been used to analyze the transient radiant transfer in oceanographic lidar.<sup>9</sup> The DOM in conjunction with the piecewise parabolic method scheme used previously to obtain numerical solutions for two-dimensional scattering-absorbing medium is used in this paper.<sup>42</sup>

No previous study has been reported in the literature which compares the experimentally measured scattered optical signals from a tissue medium containing tumors / inhomogeneities due to short pulse laser irradiation with accurate numerical solutions of transient radiative transport equation. Such studies are critical for predicting the optical properties of tissues from temporal scattered optical signal measurements. In this paper the temporal optical transmitted and reflected signals from tissue phantoms without and with inhomogeneities imbedded in it are measured with a streak camera. Parametric study involving different scattering and absorption coefficients of tissue phantoms and inhomogeneities as well as the detector position and orientation is performed. The experimentally measured temporal scattered optical signals are compared with numerical modeling results obtained by solving the transient radiative transport equation using the discrete ordinates method.

## 2. MATHEMATICAL FORMULATION

In this paper the tissue medium is approximated by an anisotropically scattering and absorbing rectangular enclosure in which a tumor / inhomogeneity is imbedded in it (see Figure 1). The transient radiative transfer equation (RTE) in a given direction  $\Omega$  is given by<sup>15,43</sup>:

$$\frac{1}{c} \frac{\partial I(x, y, \Omega, t)}{\partial t} + \mu \frac{\partial I(x, y, \Omega, t)}{\partial x} + \eta \frac{\partial I(x, y, \Omega, t)}{\partial y} + k_e I(x, y, \Omega, t) = \frac{k_s}{4\pi} \int_{4\pi} \Phi(\Omega', \Omega) I(x, y, \Omega', t) d\Omega' + S(x, y, \Omega, t) \quad (1)$$

where  $I$  is the scattered diffuse intensity ( $\text{Wm}^{-2}\text{sr}^{-1}$ ),  $k_e$  and  $k_s$  are the extinction coefficient and the scattering coefficient respectively,  $\Phi$  is the phase function,  $\Omega$  the direction cosine,  $c$  is the velocity of light in the medium,  $x$  and  $y$  are the spatial coordinates,  $t$  is the time, and  $S$  is the source term.

The scattering phase function can be represented in a series of Legendre polynomials  $P_n$  by:

$$\Phi(\Omega', \Omega) = \sum_{n=0}^N (2n+1) g^n P_n[\cos(\Theta)] \quad (2a)$$

where  $g$  is the asymmetry factor. Higher the value of  $g$ , more forward scattered is the phase function of the medium. Tissues usually are highly forward scattered medium. The scattering angle  $\Theta$  is represented by:

$$\cos(\Theta) = \mu\mu' + \eta\eta' + \xi\xi' \quad (2b)$$

where  $\mu$ ,  $\eta$ , and  $\xi$  are the directions cosines of the light propagation direction  $\Omega$ .

The pulsed radiation incident on the tissue medium at face 1 (see Figure 1) is a Gaussian-shaped pulse having a temporal duration (pulse width)  $t_p$  at full width half-maximum (FWHM). The intensity can be separated into a collimated component, corresponding to the incident source, and a scattered intensity. If  $I_c$  is the collimated intensity, then  $I$  is the remaining intensity described by Eq. (1). The collimated component of the intensity for the square pulse is represented by:

$$I_c(x, y, \Omega, t) = I_0 e^{-k_e x} [H(t - x/c) - H(t - t_p - x/c)] \delta(\Omega - \Omega_0) \quad (3)$$

where  $I_0$  is the intensity leaving the wall towards the medium,  $H(t)$  the Heaviside step function, and  $\delta(t)$  the Dirac delta function. The Gaussian pulse is approximated as a square pulse for ease of numerical implementation.

The source function  $S$  formed from the collimated irradiation is then given by:

$$S(x, y, \Omega, t) = \frac{k_s}{4\pi} \int_{4\pi} \Phi(\Omega', \Omega) I_c(x, y, \Omega', t) d\Omega' \quad (4)$$

The boundary conditions are such that intensity leaving the boundary surface is composed of the contribution of the outgoing emitted intensity and the reflection of incoming radiation in direction  $\Omega$ .

In the discrete ordinates method, the radiative transfer equation and the associated boundary condition are replaced with a set of equations for a finite number of  $M$  directions that cover  $4\pi$  sr solid angles. The integral terms of Eqs. (1) and (4) are reformulated with the aid of an angular quadrature of order  $M$ .

The discrete form of the time-dependent radiative transport equation in the direction  $\Omega_m$  is then represented as:

$$\frac{1}{c} \frac{\partial I_m(x, y, t)}{\partial t} + \mu_m \frac{\partial I_m(x, y, t)}{\partial x} + \eta_m \frac{\partial I_m(x, y, t)}{\partial y} = -k_e I_m(x, y, t) + \frac{k_s}{4\pi} \sum_{m'=1}^M w_{m'} \Phi_{m'm} I_{m'}(x, y, t) + S_m(x, y, t) \quad (5)$$

where  $m = -M, \dots, -1, 1, \dots, M$ ,  $\{\Omega_m, w_m\}$  defines a quadrature of  $M$  discrete directions  $\Omega_m$  to which the weights  $w_m$  are associated.

In this study, the Piecewise Parabolic Advection (PPA) scheme already developed by the authors to solve the two-dimensional geometry is used Eq. (5).<sup>34,42,44,45</sup> The left-hand-side of Eq. (5) is treated by the upwind monotonic interpolation methods. PPA scheme is very efficient and produces very small amount of diffusion.

### 3. EXPERIMENTAL PROCEDURE

Argon-Ion laser mode locked laser having a pulse width ( $t_p$ ) = 200 ps at FWHM operating at a frequency of 76 MHz and having a wavelength of 532 nm is used. Figure 2 shows the schematic of the experimental setup. The optical path length is controlled by using dielectric mirrors mounted on translation stages. Attenuators are used to control incident power on tissue phantoms. The beam is incident on the phantom and scattered transmitted and reflected signals are collected using a Hamamatsu streak camera unit. The streak unit comprises of ultra fast synchroscan unit with the frequency-tuning unit coupled with a Hamamatsu CCD camera. The streak camera image acquisition control is remotely done using the HPDTA\_32 software, which is also used for image processing. The streak camera is triggered from the mode locker at the rate of 76 MHz. The power and pulse width of the laser is monitored throughout the experiment using a powermeter and ultrafast photodiode respectively.

### 4. RESULTS

Experimental investigations of the nature of interactions of short-pulsed laser with scattering absorbing media like tissue phantoms containing inhomogeneities / tumors are conducted. The results are validated with numerical modeling results obtained by solving a two-dimensional transient radiative transport equation using the discrete-ordinates method. The tissue phantoms used are cast by mixing araldite resin having a refractive index ( $n$ ) of 1.54 together with an anhydride and a hardener. Typical sample cross-section used is 25 mm x 25 mm with varying thickness. Titanium Dioxide (TiO<sub>2</sub>) particles having a mean diameter of 0.3 μm is added as scatterers and dye is used as absorbers. The scattering and absorption coefficients are varied by varying the concentration of TiO<sub>2</sub> and dye in the resin matrix.<sup>46</sup> Nonhomogeneities typically of 4 mm diameter are drilled in the samples and filled with different scattering and absorption coefficients than the base resin matrix. Experiments are conducted on tissue phantoms to measure transmitted and reflected optical signals along the axis of the laser beam as well as at different angles. For numerical simulations a value of  $g = 0.8$  is used.

Figure 3 shows the normalized transmitted signal measurements obtained with a homogenous tissue phantom of thickness ( $L$ ) = 4 mm. The sample having a scattering coefficient ( $k_s$ ) = 17.33 mm<sup>-1</sup> and absorption coefficient ( $k_a$ ) = 0.01 mm<sup>-1</sup> is used. It is observed that the experimental result agrees with the numerical simulation results. It is observed that the experimental results and numerical simulation differs by 5 ps, which is within the uncertainty of the streak camera. The time for earliest arriving photon for the 4 mm phantom of refractive index  $n$  of 1.54 is =

$$\frac{\text{Length of the medium}}{\text{Speed of Light in the medium}} = \frac{4 \times 10^{-3} \text{ m}}{\frac{3 \times 10^8 \text{ m/s}}{1.54}} = 20.535 \text{ ps.}$$

The transmission signal values are zero till this time. These

values are consistent with both the numerical and experimental measurements as observed in Figure 3a. Many previously used approximate models fails to capture this effect and provide unrealistic results for the transmitted signals even before light has traversed through the medium.

Experiments are also conducted by varying the amount of scatterers and therefore the scattering coefficient for the case of 8 mm thick homogeneous tissue phantoms. The normalized temporal transmitted signal profiles are plotted for various scattering coefficients, keeping the absorption coefficient fixed. It is observed in Figure 4 that the temporal spread increases with the increase of concentration of scatterers in the phantoms as the phantoms undergo more multiple scattering. The magnitude of the signal also increases with the increase of the scattering coefficients but is masked due to the normalization with respect to corresponding peak intensity values. The effect of the variation of the absorption coefficient of the tissue phantom is depicted in Figure 5. Higher the absorption, higher will be the attenuation of the laser beam and hence lower the temporal broadening.

Figure 6 shows temporal profiles of normalized transmitted signal for a tissue phantom containing inhomogeneity/tumor. The scattering coefficients of healthy and tumorous tissues are different with inhomogeneity having higher scattering

coefficient than surrounding base medium. A distinct change in the temporal transmitted signal is observed compared to the results for homogeneous tissue phantom as shown in Figure 3.

Figure 7a shows numerically the non-dimensional temporal transmitted signals for different scattering coefficients of the base medium. Lower values of scattering coefficients of the tissue medium imply less attenuation of the laser intensity and hence higher magnitude of the measured signal. Also as the difference between scattering coefficients between base tissue medium and inhomogeneity increases there is an inflection in the measured signal implying the presence of some inhomogeneity in the medium. Corresponding spatial distribution of intensity along the face opposite to the incident face (2) is presented in Figure 7b at a particular time instant.

## 5. CONCLUSIONS

A comprehensive experimental and numerical investigation is performed to analyze short pulse laser propagation through tissue medium having inhomogeneities / tumor imbedded in it. Parametric study as performed in this paper is critical in order to differentiate between healthy and tumorous tissue. Accurate validation of the forward transient radiative transport equation with the experimentally measured data is critical before development of inverse algorithm. Short pulse laser probing for detection of tumors in tissues is a novel and nascent technology and this research work can be furthered by experiments on animal models.

## ACKNOWLEDGEMENTS

KM, CD, and AT acknowledge partial support from Oak Ridge National Laboratory through Contract No. 4000004751. TVD acknowledges support from NIH grant No. 1 R01 CA88787-01 and US Department of Energy, Office of Environmental and Biological Research under Contract No. DE-AC05-00OR22725 with UT Battelle, LLC.

## REFERENCES

1. S. Kumar and K. Mitra, "Microscale aspects of thermal radiation transport and laser applications," *Advances in Heat Transfer* **33**, 187-294, Academic Press, San Diego (1999).
2. S.A. Prael, M.J.C. van Gemert, and A.J. Welch, "Determining the optical properties of turbid media by using adding-doubling method," *Applied Optics* **32**, 559-568 (1993).
3. Y. Yamada, "Light-tissue interaction and optical imaging in biomedicine," *Annual Review of Fluid Mechanics and Heat Transfer (Ed: C.L. Tien)* **6**, 1-59 (1995).
4. J.C. Hebden, H. Veenstra, H. Dehghani, E.M.C. Hillman, M. Schweiger, S.R. Arridge, and D.T. Delpy, "Three dimensional time-resolved optical tomography of a conical breast phantom," *Applied Optics* **40**, 3278-3287 (2001).
5. G.J.R. Spooner, T. Juhasz, R. Imola, G. Djotyan, C. Horvath, Z. Sacks, G. Marre, D. Miller, A.R. Williams, R. Kurtz, "New developments in ophthalmic applications of ultra fast lasers Source," *SPIE-Commercial and Biomedical Applications of Ultrafast Lasers II* **3934**, 62-72 (2000).
6. J.E. Marion and B.M. Kim, "Medical applications of ultra-short pulse lasers," *SPIE- Commercial and Biomedical Applications of Ultrafast Lasers* **3616**, 42-50 (1999).
7. R.M. Kurtz, V. Elnor, X. Liu, T. Juhasz, F.H. Loesel, C. Horvath, M.H. Niemz, and F. Noack, "Plasma-mediated ablation of biological tissue with picosecond and femtosecond laser pulses," *SPIE Proceedings* **2975**, 192-200 (1997).
8. F.H. Loesel, A.C. Tien, S. Backus, H. Kapteyn, R. M. Murane, S. Sayegh, T. Juhasz, "Effect of reduction of laser pulse width from 100 ps to 20 fs on the plasma-mediated ablation of hard and soft tissue," *SPIE-Thermal Therapy, Laser Welding, and Tissue Interaction* **3565**, 116-123 (1999).

9. K. Mitra, and J.H. Churnside, "Transient radiative transfer equation applied to oceanographic lidar," *Applied Optics* **38**, 889-895 (1999).
10. R.E. Walker and J.W. McLean, "Lidar equations for turbid media with pulse stretching," *Applied Optics* **38**, 2384-2397 (1999).
11. M. Gower, "Excimer laser microfabrication and micromachining," *SPIE 1st International Symposium on Laser Precision Microfabrication*, **4088**, 124-131(2000).
12. A. Yodh, and B. Chance, "Spectroscopy and Imaging with Diffusing Light," *Physics Today* **48**, 34-40 (1995).
13. E.C. Hillman, J.C. Hebden, M. Schweiger, H. Dehghani, F.W. Schmidt, D.T. Delpy, and S.R. Arridge, "TimerResolved optical tomography of the human forearm," *Physics in Medicine and Biology* **46**, 1117-1130 (2001).
14. O. Jarlman, R. berg, S. Andersson-Engels, S. Svanberg, and H. Pettersson, "Time-resolved white light transillumination for optical imaging," *Acta Radiologica* **38**, 185-189 (1997).
15. K. Mitra and S. Kumar, "Development and Comparison of models for light pulse transport through scattering absorbing media," *Applied Optics* **38**, 188-196 (1999).
16. D.J. Hall, J.C. Hebden, and D.T. Delpy, "Imaging very-low-contrast objects in breastlike scattering media with a time-resolved method," *Applied Optics* **36**, 7270-7276 (1997).
17. A.H. Hielscher, D.M. Catarious, A. Klose, and K.M. Hanson, "Tomographic imaging of brain and breast tissue by time-resolved model-based iterative image reconstruction," *Proceedings of Advances in Optical Imaging and Photon Migration*, 125-127 (1998).
18. S.R. Arridge, "The forward and inverse problem in time resolved infrared imaging," *Medical Optical Tomography: Functional Imaging and Monitoring (Ed: G. Muller)* SPIE Press, Bellingham (1993).
19. J.R. Singer, F.A. Grunbaum, P. Kohn, and J.P. Zubelli, "Image reconstruction of the interior of bodies that diffuse radiation," *Science* **248**, 990-991 (1990).
20. K.M. Yoo, and R.R. Alfano, "Time-resolved coherent and incoherent components of forward light scattering in random media," *Optics Letters* **15**, 320-322 (1990).
21. K.M. Yoo, B.B. Das, F. Liu, Q. Xing, and R.R. Alfano, "Femtosecond time-gated imaging of translucent objects hidden in highly scattering media," *Springer Series in Chemical Physics* **55**, 124-127 (1993).
22. J.C. Hebden, R.A. Kruger, K.S. Wong, "Tomographic imaging using picosecond pulses of light," *SPIE Proceedings Medical Imaging V: Image Physics* **1443**, pp. 294-300 (1991).
23. L. Wang, P.P. Ho, C. Liu, G. Zhang, and R.R. Alfano, "Ballistic 2-D imaging through scattering walls using an ultrafast kerr gate," *Science* **253**, 769-771 (1991).
24. R.R. Alfano, X. Liang, L. Wang, and P.P. Ho, "Time resolved imaging of translucent droplets in highly scattering turbid media," *Science* **264**, 1913-1915 (1994).
25. R. Berg, S. Andersson-Engels, O. Jorlman, and S. Svanberg, "Time-resolved transillumination for medical diagnostics," *SPIE Proceedings* **1431**, 110-119 (1991).
26. D. Huang, E.A. Swanson, C.P. Lin, J.S. Schuman, W.G. Stinson, W. Chang, M.R. Hee, T. Flotte, K. Gregory, C.A. Puliafito, and J.G. Fujimoto, "Optical coherence tomography," *Science* **254**, 1178-1181 (1991).

27. J.C. Hebden, "Evaluating the spatial resolution performance of time-resolved optical imaging system," *Medical Physics* **19**, 1081-1087 (1992).
28. H. Jiang, K.D. Paulsen, U.L. Osterberg, B.W. Pogue, and M.S. Patterson, "Simultaneous reconstruction of optical absorption and scattering maps in turbid media from near-infrared frequency-domain data," *Optics Letters* **20**, 2128-2130 (1995).
29. E. Gratton, W.M. Mantulin, M.J. vande Ven, J.B. Fishkin, M.B. Maris, and B. Chance, "A novel approach to laser tomography," *Bioimaging* **1**, 40-46 (1993).
30. K.W. Berndt and J.R. Lakowicz, "Detection and localization of absorbers in scattering media using frequency domain principles," *SPIE Proceedings* **1431**, 149-160 (1991).
31. M.A. O'Leary, D.A. Boas, B. Chance, and A.G. Yodh, "Experimental images of heterogeneous turbid media by frequency domain diffusing photon tomography," *Optics Letters* **20**, 426-428 (1995).
32. M.Q. Brewster, and Y. Yamada, "Optical properties of thick turbid media from picosecond time-resolved light scattering measurement," *International Journal of Heat and Mass Transfer* **8**, 2569-2581 (1995).
33. A. Ishimaru, "Diffusion of light in turbid material," *Applied Optics* **28**, 2210-2215 (1989).
34. M. Sakami, K. Mitra, and T. Vo-Dinh, "Analysis of short-pulse laser photon transport through tissues for optical tomography," *Optics Letters*, **27**, 336-338 (2002).
35. M. Sakami, K. Mitra, P. Hsu, "Transient radiative transfer in anisotropically scattering media using monotonicity-preserving schemes," *International Mechanical Engineering Congress and Exposition* **366-1**, 135-143 (2000).
36. S. Kumar, K. Mitra, and Y. Yamada, "Hyperbolic damped-wave models for transient light-pulse propagation in scattering media," *Applied Optics* **35**, 3372-3378 (1996).
37. K. Mitra, M.S. Lai, and S. Kumar, "Transient radiation transport in participating media within a rectangular enclosure," *AIAA Journal of Thermophysics and Heat Transfer* **11**, 409-414 (1997).
38. Z.M. Tan, and P.F. Hsu, "An integral formulation of transient radiative transfer," *ASME Journal of Heat Transfer* **123**, 466-475 (2001).
39. C.Y. Wu, and S.H. Wu, "Integral equation formulation for transient radiative transfer in an anisotropically scattering medium," *International Journal of Heat and Mass Transfer* **43**, 2009-2020 (2000).
40. A.H. Gandbakche, R. Nossal, and R.F. Bonner, "Scaling relationships for theories of anisotropic random walks applied to tissue optics," *Applied Optics* **32**, 504-516 (1993).
41. A. Sawetprawichkul, P.F. Hsu, K. Mitra, and M. Sakami, "A Monte Carlo study of the transient radiative transfer within the one-dimensional multi-layered slab," *International Mechanical Engineering Congress and Symposium, Orlando (Florida)* **366-1**, 145-153 (2000).
42. M. Sakami, K. Mitra, and P.F. Hsu, "Analysis of light-pulse transport through two-dimensional scattering-absorbing media," *Journal of Quantitative Spectroscopy and Radiative Transfer* **73**, 169-179 (2002).
43. M.F. Modest, *Radiative Heat Transfer*, McGraw Hill (1993).
44. G. Strang, "On the construction and comparison of difference schemes," *SIAM Journal of Numerical Anal*s **5**, 506-517 (1968).

45. P. Colella, and P.R. Woodward, "The piecewise parabolic method for gas-dynamical simulations," *Journal of Computational Physics* **54**, 174-201 (1984).
46. M. Firbank, and D.T. Delpy, "A design for a stable and reproducible phantom for use in near infra-red imaging and spectroscopy," *Physics in Medicine and Biology* **38**, 847-853 (1993).

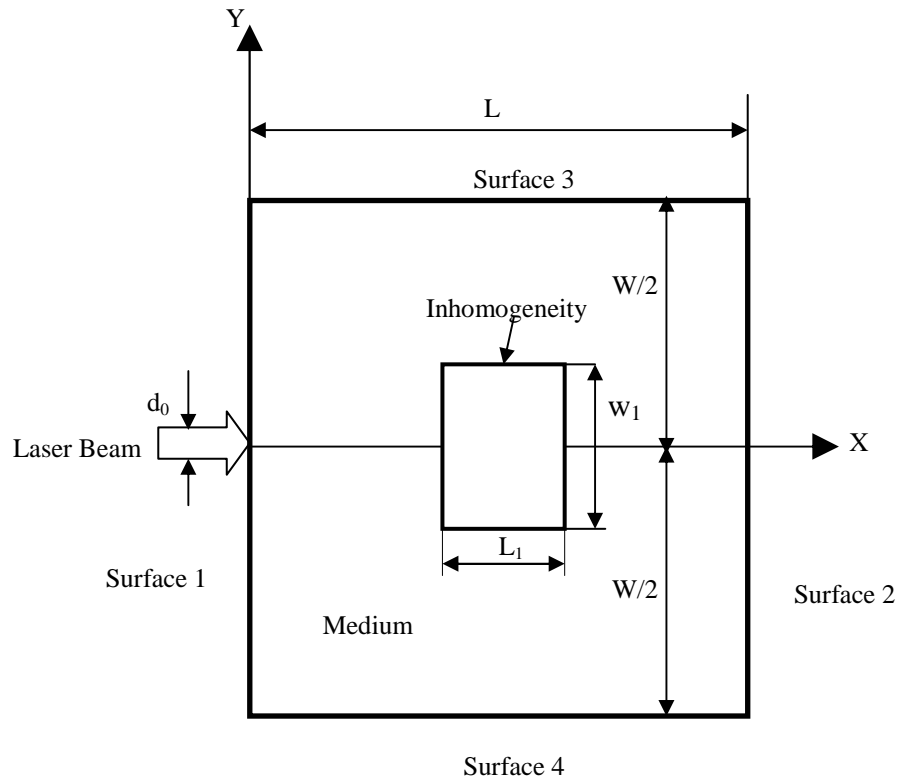


Figure 1. Schematic of the problem under consideration.

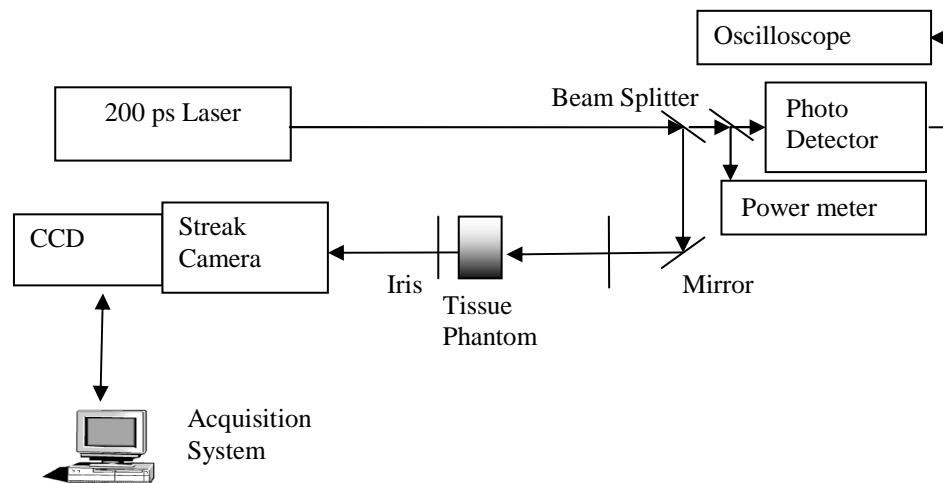


Figure 2. Schematic of the experimental setup.

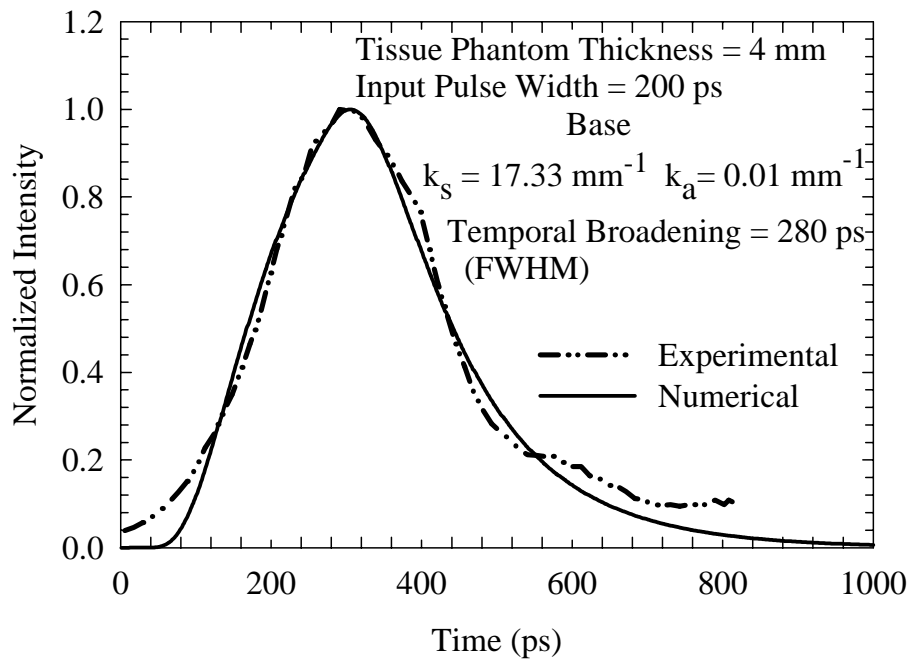


Figure 3. Temporal transmitted signal for a homogenous sample.

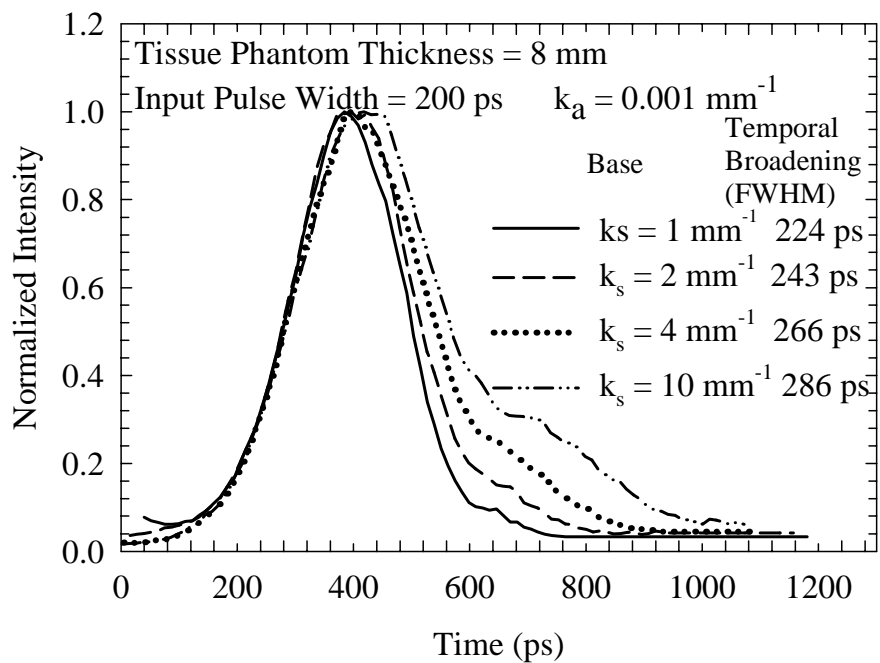


Figure 4. Effect of scattering coefficient on temporal transmitted signal for a homogeneous sample.

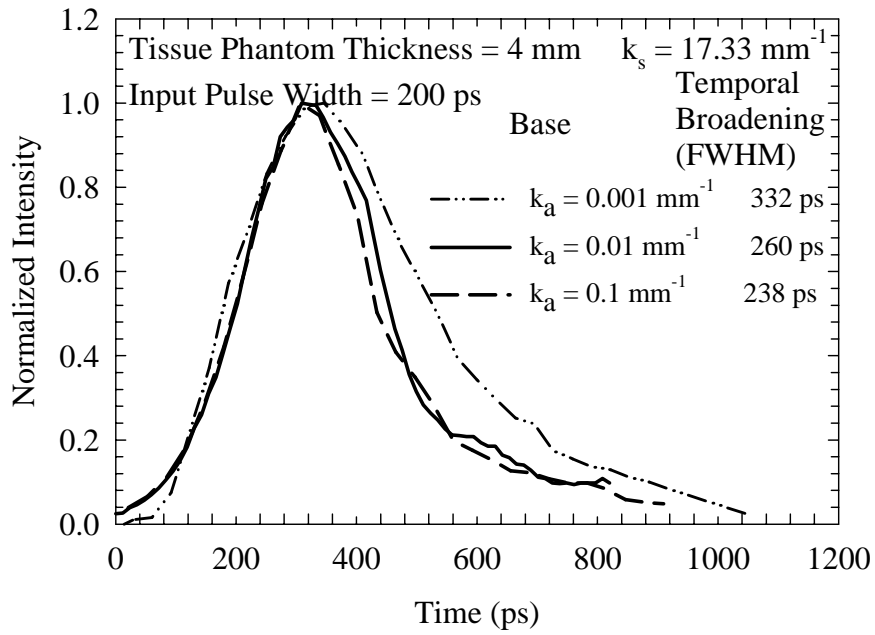


Figure 5. Effect of absorption coefficient on temporal transmitted signal for a homogeneous sample.

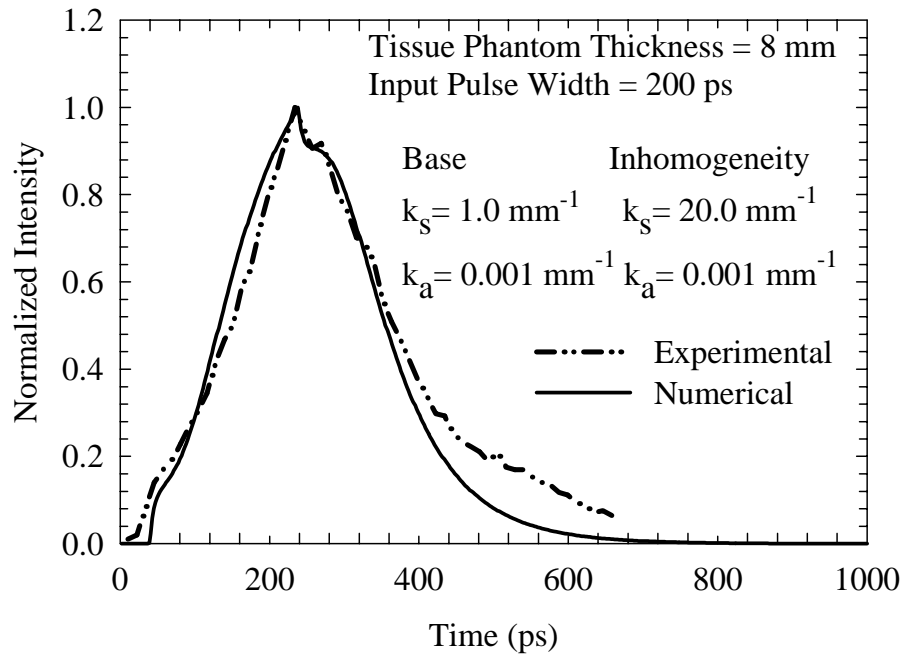


Figure 6. Transmitted signal through a phantom containing inhomogeneity.

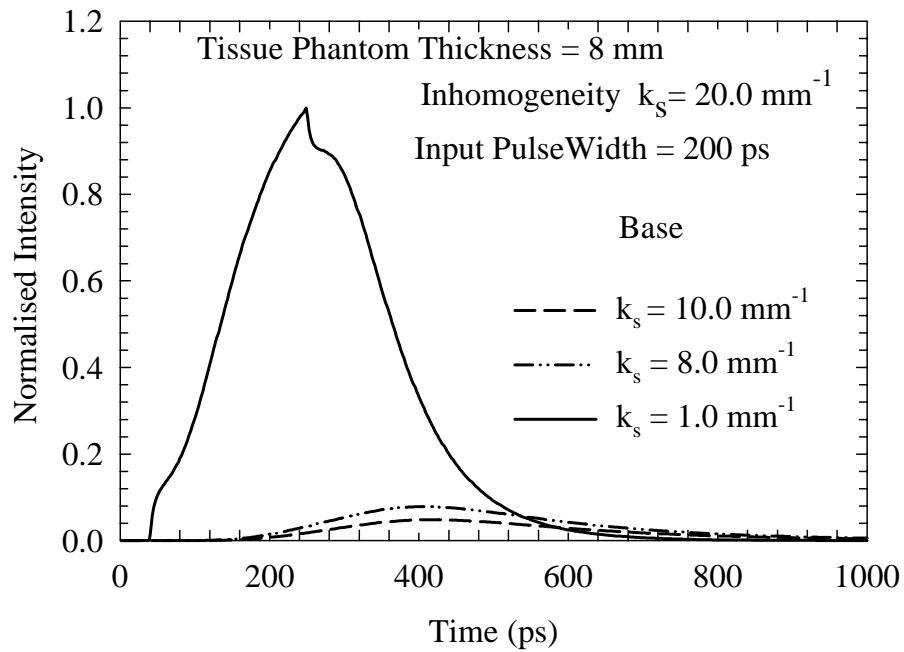


Figure 7a. Temporal transmitted signals for various scattering coefficient of base medium.

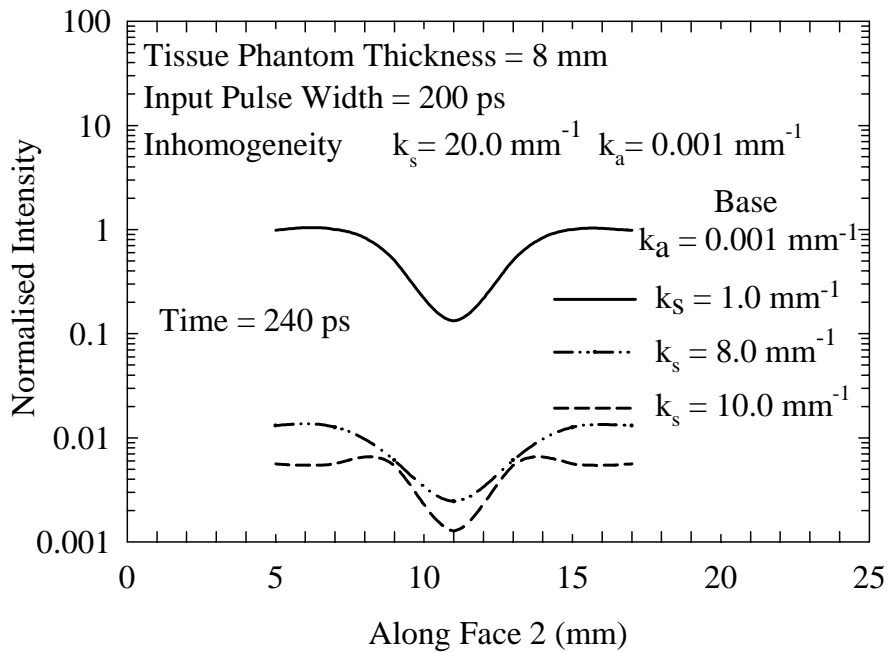


Figure 7b. Spatial distribution of intensity in the phantom for various scattering coefficients of the base medium.